International Journal of Modern Physics B
Vol. 25, No. 1 (2011) 55–71

DOI: 10.1142/S0217979211056275

World Scientific
www.worldscientific.com

THE PROPERTIES OF PROTON CONDUCTIVITY ALONG THE HYDROGEN-BONDED MOLECULAR SYSTEMS WITH DAMPING UNDER INFLUENCES OF THERMAL PERTURBATION AND STRUCTURE NONUNIFORMITY

PANG XIAO-FENG*,†, YU JIA-FENG* and ZENG HONG-JUAN*

*Institute of Life Science and Technology,
University of Electronic Science and Technology,
Chengdu 610054, P.R. China
†International Centre for Materials Physics,
Chinese Academy of Sciences, Shenyang 110015, P.R. China
†pangxf@mail.sc.cninfo.net

Received 3 September 2008

The effects of structure nonuniformity and thermal perturbation on properties of proton conductivity in hydrogen-bonded systems with damping exposed in an externally applied electric-field have been numerically studied by fourth order Runge–Kutta method in our soliton model. The results obtained show that the proton-soliton is very robust against the structure disorder including the fluctuation of the force constant and disorder in the sequence of masses and thermal perturbation and damping effect of medium, its velocity of conductivity increases with increasing externally applied electric-field and with decreasing damping coefficient of medium, but the proton-soliton disperses at quite great fluctuations of force constant and damping coefficient. In the meantime, the proton-soliton in ice crystals is thermally stable in the region of temperature of $T \leq 273$ K. From the numerical simulation, we find out that the mobility (or velocity) of proton conduction in ice is a nonmonotonic function of temperature in the temperature region of 170–273 K, i.e., it increases initially, reaches a maximum at about 191.4 K, subsequently decreases to a minimum at about 211.6 K, and then increases again. This changed rule of mobility obtained consists qualitatively with its experimental datum in ice in the same temperature region. Thus these results provide an evidence for the soliton excited in the hydrogen-bonded systems.

Keywords: Hydrogen bond; proton transfer; structure nonuniformity; thermal perturbation; mobility; Runge–Kutta method.

PACS numbers: 03.65.-w, 33.20.kf, 66.30.Dn, 82.39.Jn

1. Introduction

It is well-known that ice, lithium hydrazinium sulfate, imidazole, crystalline hydrogen halides and proteins are some typically hydrogen-bonded molecular systems. The prototype of the systems can be represented by a series of hydrogen bonds as $\cdots \mathrm{X}-\mathrm{H}\cdots\mathrm{X}.\ -\mathrm{H}\cdots\mathrm{X}-\mathrm{H}\cdots$, where X is a heavy ion or OH in ice or N—C═O

in proteins.[1–8] It is a well-established fact that the hydrogen ions or protons are the dominant charge carriers and the hydrogen-bonded chains provide a channel for the proton transport. Experimental investigations of conductivity show that the proton conductivity along the direction of the channel is 1000 times larger than that in the perpendicular directions. Its mobility is comparable to the electronic mobility in some semiconductors. For this reason, these materials have been termed "protonic semiconductors". Ice crystal is a convenient type of proton transfer in the hydrogen-bonded molecular systems. Eigen and Maeyer[4] reported an observation of high-mobility ($\sim 0.05 - 0.1$ m^2/Vs) of proton transfer in ice. However, lower protonic mobility was found later by Nagle[5,6] in ice which supports the belief that earlier reported mobility might have been the result of surface conduction. Recently reported values are on the order of $\sim (5 - 10) \times 10^{-3}$ cm^2/Vs. These, however, are still many orders of magnitude larger than the mobilities of other ions such as Li^+ and F^- in ice.[4]

Obviously, the high efficiency of proton transport in the hydrogen-bonded systems is associated with possible coherence features in the proton motions. The cooperative proton dynamics in these networks can be directly attributed to the proton-proton interaction and the nonlinear nature of the hydrogen bond chains. Because of the symmetry of an isolated oxygen-proton-oxygen complex in ice, thus the effective potential of protons has the form of a double well. Two symmetric equilibrium positions of hydrogen ions are separated by a potential barrier and the height of the barrier depends strongly on the distance between the adjacent X atoms. The properties of the proton potential and proton-proton interaction lead naturally to the association of possible coherence in proton motions with the concept of topological solitons in the systems.[9–34] The soliton model of proton transfer in ice was first proposed by Ankonchenko *et al.* (ADZ model).[9] In this model the protons in the hydrogen bonds of the chain become a soliton through the double-well potential, and the coupling between the proton and X atoms provide a barrier-lowering mechanism that allows an proton transfer between the two equilibrium positions. Thus the coupling between a vibrational proton in a double-well potential and an optical mode of the heavy ionic sublattice is included in this model. An ionic defect appears as a solitary wave in the proton sublattice which propagates together with a contraction of the relative distance between neighboring heavy ions. This model is further pursued in a number of works[11–41,44,45] in which a variety of theoretical extensions have been derived, some involve the one-component protonic chain with two parameters proposed by Pnevmatikos *et al.*[13,14,17,20,22] However, this model is only effective for explaining the transfer of ionic defects, and fails for the Bjerrum (or bonded) defect in the systems. Meanwhile, the dynamical equations in this model are also very difficult to solve, so that an exact analytical solution cannot also be obtained. If realistic values for the parameters of the systems are considered, the continuum approximation fails due to the narrowing of the domains of validity of the solutions with respect to the lattice spacing. The one-component

model[20–22] is not accepted because the influence of heavy ionic sublattice on the protons is not considered in detail in this model. Therefore, the proton transfer in the hydrogen-bonded systems is still an open problem.

Recently we proposed a model for the study of dynamic properties of proton transfer in hydrogen-bonded systems. In this model, the proton motion crossing the potential barrier between a pair of heavy ions is introduced. It resulted in changes of relative positions between the protons and neighboring heavy ions and occurrence of ionic defect. The interaction between the proton and heavy ion, which is weaker due to larger separation between them, reduce only the height of the barrier that the proton has to overcome to pass from one well to the other. However, when the protons approach the neighboring heavy ions, the above interaction is greatly enhanced and can be so much stronger than the double-well potential that the protons can cross over the barrier and move from one side to the other due to this nonlinear interaction. The transfer of protons takes place via a quasi-self-trapping mechanism-deformation of heavy ionic sublattice arising from its stretching and compression. Thus, the directions of covalent bonds between the protons and heavy ions are exchanged. In other words, a rotation of bond takes place or a Bjerrum defect appears in such a case. Therefore, the interbond proton motion or rotation of the bond (Bjerrum defect), is mainly determined by the nonlinear interaction between the protons and heavy ions. Then, two types of defects, ionic and bonded, can occur through the competition of the two kinds of nonlinear interaction, the double-well potential and the nonlinear interaction. The properties of proton transfer were thus well-described in our new model.

However, the above results are obtained by analytic method in which the hydrogen-bonded system is thought to be periodic, all physical parameters of the system are used to be their average values, and some approximate methods, containing long-wave approximation and continuum approximation, and so on, are used in the calculation. In practice, the hydrogen-bonded system consists of different atomic groups with molecular weights, thus they are not periodic, but aperiodic and nonuniform. This is just so-called structure nonuniformity or disorder of hydrogen-bonded systems. The structure aperiodicity or nonuniformity is caused by the differences of particle numbers involved in the heavy ion groups in these hydrogen bonds or some impurities importing. The phenomenon occurs also in ice crystal, the structure nonuniformity here arises from the differences of numbers of water molecules which are linked with OH groups in the hydrogen bonds. Thus it is necessary to result in the fluctuations of physical parameters in the new model due to the structure nonuniformity. Hence corresponding states of soliton will be affected in the new model because the properties and states of the soliton are just determined by these physical parameters of the hydrogen bonded systems. Thus these practical problems should be studied, but have not been studied up to now. On the other hand, thanks to the hydrogen-bonded systems always working at a finite temperature, then the influences of the thermal perturbation on the proton

conductivity in the systems is also of interest. In such a case it is very necessary to study the influences of structure nonuniformity on the solitons at different temperature. However, how do we determine the effects of nonuniformity on the solitons? Since the above solitons excited in the periodic and uniform hydrogen-bonded systems are stable, then its stable states will be changed due to the fluctuations of physical parameters and thermal perturbations arising from the structure nonuniformities and temperature of the systems. Thus we can determine and judge their influences and efforts on the behaviors of the solitons in virtue of the variations of stability of the solitons in such a case relative to that in the case of periodic and uniform systems. This is just our instructive idea in this investigation. In this paper we study mainly the states and features of soliton in the nonuniform and aperiodic hydrogen-bond systems and calculate the temperature-dependences of mobility of proton conductivity by numerical simulation and fourth order Runge-Kutta method in the new model, in which we here consider not the influences of quantum effects of protons, a lightest nucleus, on the states of the solitons, which complicates our studied problem. We will see from this investigation that not only the soliton is still thermally stable at different temperatures and very robust against these structure nonuniformities of the systems, but also its mobility has some novel features. In Sec. 2, we introduce the Hamiltonian of the systems and give corresponding dynamic equations in the new model; the properties of motion of the solitons in the nonuniform hydrogen-bonded systems at different temperatures are described in Sec. 3. In Sec. 4 we state the conclusion of this paper.

2. The Hamiltonian of Systems and Corresponding Dynamic Equations

In the new model we have included a double-well potential of proton represented by $U(R_n) = U_0[1-(R_n/R_0)^2]^2$, the elastic interaction caused by the covalent interaction, the coupled interaction between the protons and heavy ions, the resonant or dipole-dipole interaction between neighboring protons and changes of relative positions of neighboring heavy ions resulting from the resonant interaction. If assuming again the harmonic model for acoustic vibrations of the heavy ionic sublattice, the Hamiltonian of the systems can be written as

$$\begin{aligned} H &= H_p + H_{\text{ion}} + H_{\text{int}} \\ &= \sum_n \left[\frac{1}{2m} p_n^2 + \frac{1}{2} m\omega_0^2 R_n^2 - \frac{1}{2} m\omega_1^2 R_n R_{n+1} + U_0 \left[1 - \left(\frac{R_n}{R_0} \right)^2 \right]^2 \right] \\ &\quad + \sum_n \left[\frac{1}{2M} P_n^2 + \frac{1}{2} W(u_n - u_{n-1})^2 \right] \\ &\quad + \sum_n \left[\frac{1}{2} \chi_1 m(u_{n+1} - u_{n-1}) R_n^2 + m\chi_2 (u_{n+1} - u_n) R_n R_{n+1} \right] \end{aligned} \tag{1}$$

where the proton displacement and momentum are R_n and $p_n = mR_n$, respectively, the first being the displacement of hydrogen atom from the middle of the bond between the nth and the n+1th heavy ions in the static case. R_0 is the distance between the central maximum and one of minima of double-well potential, U_0 is the height of barrier of double-well potential. Similarly, u_n and $P_n = Mu_n$ are the displacement of heavy ion from its equilibrium position and its conjugate momentum, respectively. $\chi_1 = \partial\omega_0^2/\partial u_n$ and $\chi_2 = \partial\omega_1^2/\partial u_n$ are coupling constants between the proton and heavy ion sublattices, and represent the changes of energy of vibration of protons and of coupled energy between neighboring protons due to an unit extension of heavy ionic sublattice, respectively. $(1/2)m\omega_1^2 R_n R_{n+1}$ shows the correlation interaction between neighboring protons caused by the dipole-dipole interactions. ω_0 and ω_1 are diagonal and nondiagonal elements of dynamic matrix for the proton, respectively. ω_0 is also the Einstein resonant frequency of protonic sublattice. W is the elastic constant of heavy ionic sublattice. m and M are the masses of proton and heavy ion, respectively. The part H_P of H is the Hamiltonian of protonic sublattice with an on-site double-well potential $U(R_n)$, H_{ion} is the Hamiltonian of heavy ionic sublattice with low-frequency harmonic vibration, and H_{int} is the interaction Hamiltonian between the protonic and heavy ionic sublattices. Obviously, the new model is significantly different from the ADZ model[7] and Pnevmatikos *et al.*'s models.[11,12,15,18,19] (1) Since the total mass of the heavy ion, which contains the large number of atoms or atomic groups, is large, then its motion is represented by a harmonic oscillator with low-frequency acoustic-vibration in the new model, but there are both acoustic and optical vibrations for the heavy ions in ADZ model. (2) For the motion of the proton lain in the double-well potential, we adopt the harmonic oscillator model with optical vibration that includes an off-diagonal factor arising from the interaction between neighboring protons and the interaction of proton with heavy ions. That is, its vibrational frequencies are related to displacements of heavy ions which are given by

$$\omega_0^2(u_n) \approx \omega_0^2 + \frac{\partial\omega_0^2}{\partial R_n}(u_n - u_{n-1})$$

$$= \omega_0^2 + \chi_1(u_n - u_{n-1}), \omega_1^2(u_n) \approx \omega_1^2 + \chi_2(u_n - u_{n-1})\,.$$

If inserting them into the above protonic Hamiltonian, and again taking into account the effects of neighboring heavy ions in left-and right-hand sides of protons, it is natural to obtain Eq. (1). Therefore there are high corresponding relations for these interactions in the above Hamiltonian. However, in the ADZ's Hamiltonian, the vibration of proton is acoustic. This is undesirable for the protonic model because the vibrational frequency of proton is very high relative to heavy ion due to its light mass. Moreover, there are not the above correspondent relation between the protonic and interactional Hamiltonians in the ADZ model. These problems result in some difficulties for the ADZ model. In the new model, the Hamiltonian includes not only the optical vibration of protons, but also the resonant interaction and the changes of the relative displacement of neighboring heavy ions. Therefore

the new model gives a more reasonable description of the dynamic features of the systems than the ADZ model.

Utilizing the new model we suggest that motion of proton between a pair of heavy ions crossed over the barrier in the intrabond, which results in a change of relative position between the proton and neighboring heavy ions and the occurrence of ionic defect, is mainly determined by the double-well potential. The coupled interaction between the proton and heavy ion, which is weaker due to larger spacing between them, can only reduce the height of barrier of double-well potential that the proton has to overcome to pass from one well to another. However, when the protons approach the neighboring heavy ions, the above coupled interaction will be greatly enhanced and can be so much larger than the double-well potential that the proton can shift over the barriers in the interbonds at the heavy ions from one side to another by this nonlinear coupling interaction in virtue of the mechanism of deformation of heavy ionic sublattice, arising from its stretching and compression (this is just so-called quasi-self-trapping mechanism). Thus, the direction of covalent bond between the proton and heavy ion is changed and a rotation of bond or Bjerrum defect appears. In such a case, the motion of protons crossed over the barriers in interbonds at the heavy ions, or speaking, the rotation of bond (Bjerrum defect), is mainly caused by the coupled interaction between the protons and heavy ions. Therefore, both kinds of defects, ionic and bonded, can occur through the competition of the above two kinds of nonlinear interaction, double-well potential and nonlinear coupled interaction, in the new model. Thus the properties of proton transfer via the ionic and bonded defects were well-described by the new model. At the same time, the mobility and conductivity of proton transfer obtained from this theory is also consistent with experimental results in ice crystal. Therefore, we can use the new model to study the states and features of soliton in the nonuniform and aperiodic hydrogen-bond systems and calculate the temperature-dependences of mobility of proton conductivity by numerical simulation and fourth order Runge–Kutta method.

Based on the Hamilton equations:

$$\frac{\partial}{\partial t}p_n = -\frac{\partial H}{\partial u_n}\,, \quad \text{and} \quad \frac{\partial}{\partial t}P_n = -\frac{\partial}{\partial R_n}H\,,$$

we can get the equations of motion of proton and heavy from Eq. (1) as follows

$$\begin{aligned} -m\ddot{R}_n = {} & m\omega_0^2 R_n - \frac{m\omega_1^2}{2}(R_{n+1}+R_{n-1}) + m\left[\chi_1(u_{n+1}-u_{n-1}) - \frac{4U_0}{mR_0^2}\right]R_n \\ & + m\chi_2[(u_{n+1}-u_n)R_{n+1} + (u_n-u_{n-1})R_{n-1}] + \frac{4U_0}{R_0^4}|R_n|^2 R_n \end{aligned} \tag{2}$$

and

$$\begin{aligned} M\ddot{u}_n(t) = {} & W(u_{n+1}+u_{n-1}-2u_n) + m\chi_1/2(|R_{n+1}|^2 - |R_{n-1}|^2) \\ & + m\chi_2(R_{n+1}R_n - R_nR_{n-1})\,. \end{aligned} \tag{3}$$

Equations (2)–(3) can be represented as the following forms

$$\dot{R}_{n,t} = y_{n,t}/m \tag{4}$$

$$\begin{aligned}\dot{y}_{n,t} = &-m\omega_0^2 R_{n,t} + m\omega_1^2(R_{n+1,t} + R_{n-1,t})/2 + 4U_0 R_0^{-2}(1 - (R_{n,t}/R_0)^2)R_{n,t} \\ &- m\chi_1(u_{n+1,t} - u_{n-1,t})R_{n,t} - m\chi_2[(u_{n+1,t} - u_{n,t})R_{n+1,t} \\ &+ (u_{n,t} - u_{n-1,t})R_{n-1,t}]\end{aligned} \tag{5}$$

$$\dot{u}_{n,t} = \frac{z_{n,t}}{M} \tag{6}$$

$$\begin{aligned}\dot{z}_{n,t} = &W(u_{n+1,t} + u_{n-1,t} - 2u_{n,t}) + m\chi_1(R_{n+1,t}^2 - R_{n-1,t}^2) \\ &+ m\chi_2(R_{n,t}R_{n+1,t} - R_{n,t}R_{n-1,t})\,.\end{aligned} \tag{7}$$

The above equations (4)–(7) can determine the states and behaviors of the new soliton. There are four equations for one atomic group. Hence for the hydrogen bonded system constructed by N atomic groups, there are $4N$ associated equations. When the fourth-order Runge–Kutta method is used to numerically calculate the solutions of the above equations, we should discretize them. Thus the site of atomic group is denoted by n, the time is denoted by t. The system of units eV for energy, Å for length, and ps for time proved to be suitable for the numerical solutions of Eqs. (4)–(7). In the numerical simulation by fourth-order Runge–Kutta way, we also require that the following conditions must be satisfied, the total energy E must be a constant (up to 0.0012%); the norm is conserved up to 0.3 pp (parts per million). An initial excitation is required in this calculation, it is chosen as $R_n(t=0) = A\tanh[(n-n_0)\hbar(\chi_1+\chi_2)^2/4\omega_0\omega_1^2 W]$ for the proton at nth site, where A is normalization constant, and $u_n(0) = 0$ for the heavy ion. In the meanwhile, the molecular chain in the systems is fixed, in which contained number of particle, N, is chosen to be $N = 100$, a time step size of 0.0195 is used in the simulation. Total numerical simulation is performed by data parallel algorithm and MATLAB language.

3. Numerical Calculation Results and Discussion

3.1. *Calculated results for the uniform and periodic hydrogen-bond chains*

As ice is a typically hydrogen-bonded molecular system, we always choose the ice as a model system to study the properties of proton transfer in the hydrogen-bonded

Table 1. The average values of physical parameters in ice crystal.

W (N/m)	M (kg)	R_0 (10^{-10} m)	U_0 (10^{-20} J)	ω_0 (10^{+14} s^{-1})	ω_1 (10^{14} s^{-1})	χ_1 (10^{+38}/ms^2)	χ_2 (10^{+37}/ms^2)
0.015	17 m_p	1	3.52	1.2 − 1.5	1.1 − 1.4	0.5214	3.0057

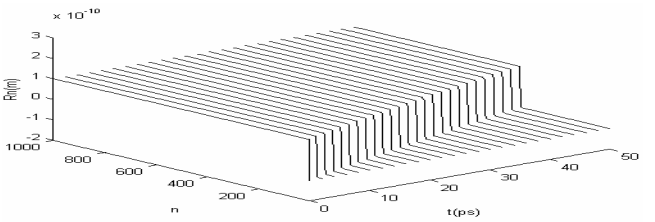

Fig. 1. The numerical solution of Eqs. (4)–(7) in ice.

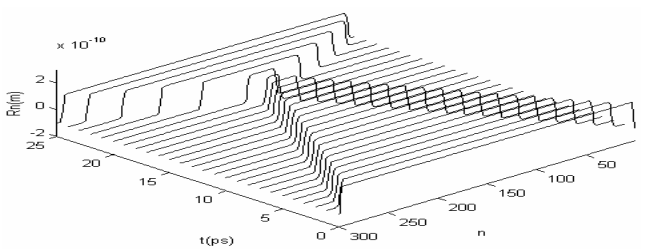

Fig. 2. The collision behavior of two solitons of Eqs. (4)–(7) in ice.

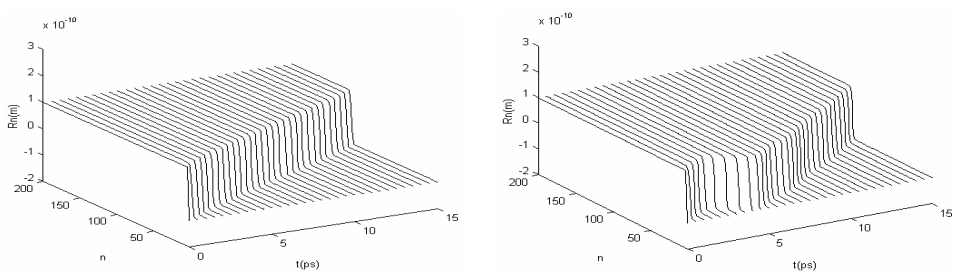

(a) (b)

Fig. 3. The states of the new soliton resulting from the fluctuations of force constant W for (a) $\Delta W = \pm 20\%\bar{W}$, (b) $\pm 30\%\bar{W}$, (c) $\pm 40\%\bar{W}$, (d) $\pm 50\%\bar{W}$ at $(-1.1 \leq \alpha_k \leq +1.1)$.

systems. Utilizing the average values of parameter, $\bar{M}$, $\bar{U}_0$, ϖ_0, ϖ_1, $\bar{W}$, $\bar{J}$, $\bar{\chi}_1$ and $\bar{\chi}_2$, shown in Table 1 for the ice, here $m = m_P$, we calculate numerically the solution of Eqs. (4)–(7) by fourth-order Runge–Kutta method in an uniform and periodic hydrogen bonded systems. This result is shown in Fig. 1. This figure shows that the amplitudes of solutions of Eqs. (4)–(7) can always retain a constancy. In Fig. 2 we show the collision property of two solutions. From these figures, we see that the two solitons can cross with each other after the collision. These results show that the equations in Eqs. (2)–(3) have exact soliton solution in the uniform and periodic systems in the new model, the soliton is a kink and quite stable. This result is consistent with that in analytic case.

3.2. *Influences of fluctuation of force constant and disorder in the sequence of mass on the new soliton*

We now use the fourth-order Runge–Kutta method to study numerically the influences of fluctuation of force constant W and variation of mass of heavy ion or atomic group, M, arising from the structure nonuniformity or impurity importing, on the stability of the soliton in the hydrogen bonded systems in the new model. In fact, the fluctuation of W is caused by the nonuniformity of distribution of masses of heavy ion groups in hydrogen bonded systems as mentioned above. To test the stability of the new soliton against the nonuniformity, we should first use a random number generator to produce or represent the random sequences of different parameters in the structure nonuniform systems. In the sequence of masses we here introduce a random number generator, α_k, to create random sequences of masses of heavy ion, thus there is a random series of masses for the whole chain, $M_k = \alpha_k \bar{M}$, where the α_k were determined using a random-number generators with equal probability within a prescribed interval. The fluctuation of W, arising from the structure nonuniformity, is designated by $\Delta W = \pm\beta\bar{W}$, $\beta < 1$. When the effects of structure nonuniformity are taken into account, the states and features of the new soliton will be changed. The results of simulations are shown in Fig. 3 for four cases of fluctuation of W at $-1.1 \leq \alpha_k \leq +1.1$. From this figure, we see that up to a random variation of $\pm 30\%\bar{W}$ we find no change in the dynamics for the new soliton. For $\pm 40\%\bar{W}$ the soliton begins to disperse, its velocity is diminished as compared with the case of $\bar{W}$ in Fig. 1. Finally, for $\pm 50\%\bar{W}$ it disperses and the propagation is irregular. Therefore we conclude that in the case of $W < \pm 40\%\bar{W}$ at $-1.1 \leq \alpha_k \leq +1.1$, virtually no change for the stability of new soliton can be obtained. Therefore the ability of the new soliton against the fluctuations of force constant and the disorder in the sequence of masses is robust.

Also, from the numerical simulations using the fourth-order Runge–Kutta method, we find that the influences of fluctuations of other physical parameters, for example, $\bar{U}_0$, ϖ_0, ϖ_1, $\bar{J}$, $\bar{\chi}_1$ and $\bar{\chi}_2$, on the properties of the new soliton are small in the new model, thus we here list not these results.

3.3. *Influences of temperature and damping of medium on the new soliton exposed in an externally applied electric-field*

Since the hydrogen-bonded systems always work in an environment (or heat bath) with finite temperature, thus it is very necessary to further study the influences of the thermal perturbation on the state and properties of the new soliton in the systems with damping. In this case we can safely assume that the heat bath primarily affects the soliton motion via the heavy ion sublattice in accordance with general rule.[36–43] According to the thermodynamic theory, a decay term $M\Gamma\dot{q}_n$ and a random thermal-noise term, $F_n(t)$, resulting from the interaction of the heat bath with temperature T with the hydrogen-bonded systems, must be added in the displacement equation of heavy ion.[36–43] If considering again the influence of

externally applied electric-field (its strength is E) on the soliton, then Eqs. (2)–(3) become

$$\begin{aligned} m\ddot{R}_n = &-m\omega_0^2 R_n + m\omega_1^2(R_{n+1}+R_{n-1})/2 + 4U_0 R_0^{-2}(1-(R_n/R_0)^2)R_n \\ &- m\chi_1(u_{n+1}-u_{n-1})R_n - m\chi_2[(u_{n+1}-u_n)R_{n+1} \\ &+ (u_n-u_{n-1})R_{n-1}] + qE \end{aligned} \tag{8}$$

$$\begin{aligned} M\ddot{u}_n = &W(u_{n+1}+u_{n-1}-2u_n) + m\chi_1(R_{n+1}^2 - R_{n-1}^2) \\ &+ m\chi_2(R_nR_{n+1} - R_nR_{n-1}) - M\Gamma\dot{u}_n + F_n(t) \end{aligned} \tag{9}$$

where Γ is the damping coefficient of medium, and is about 10^9 s^{-1} for the ice, q is the charge of proton. In this case we must give the explicit expression of random noise force $F_n(t)$. From statistical physics we know that $F_n(t)$ is related to the temperature of the systems, the average value of it is correlation function can be represented as $\langle F(x,t)F(0,0)\rangle = 2MK_BJ\delta(x)\delta(t)/r_0$, where r_0 is the lattice constant.[36–43] Since time discretization effects the properties of the Langevin forces in the numerical simulations, we here use an ensemble of Gaussian forces F_n with variance equal to $\sigma = 2MK_BT\Gamma/\tau_1$, where τ_1 is a time constant. This choice of Gaussian width is compatible with the fluctuation-dissipation theorem and time discretization.[36–43] Thus we can determine that the criterion deviation of $F_n(t)$ is $\sqrt{\sigma}$, then its expected value is zero in this case. Thus, the size of random noise force has the following relation, $|F_n(t)| \leq 6\sqrt{\sigma}$. Hence, $F_n(t)$ is Gaussian distribution at $L \to \infty$.

Utilizing Eqs. (8)–(9) we can study the influences of damping and random thermal-noise forces of medium exposed in an externally applied electric-field, E, on the states of the soliton in ice by the above fourth-order Runge–Kutta method in the new model. We here first study the effect of electric-field on the soliton at $T = \Gamma = 0$. In this case, the states of the soliton at $E = 100$ kV/cm and 200 kV/cm are shown in Fig. 4. From this figure we see that the soliton is stable, but its velocity is changed. This electric-field dependence of velocity of the soliton is shown in Fig. 5. Namely the velocity increases linearly with increasing electric-field. This is very similar with the feature of motion of macroscopic charge exposed in an electric-field. Therefore this is an interesting result. We further calculate the influence of damping of medium on the soliton in the case of $T = E = 0$. The properties of the soliton at two different damping coefficients are shown in Fig. 6. We see from this figure that no change in the stability of new soliton is found for small damping, but at great damping the soliton disperses, its velocity decreases with increase of damping coefficient, which is shown in Fig. 7. When $\Gamma \neq 0$, $T \neq 0$ and $E \neq 0$, the states of the soliton differ from the above results. In Figs. 8–9 we give the features of the soliton for four different temperatures, $T = 190$ K, 210 K and 273 K at $E = 200$ kV/cm and 100 kV/cm and $\Gamma = 2 \times 10^9$ s^{-1} in the ice, respectively. From this result we find no variation in the dynamics for the soliton under the influences

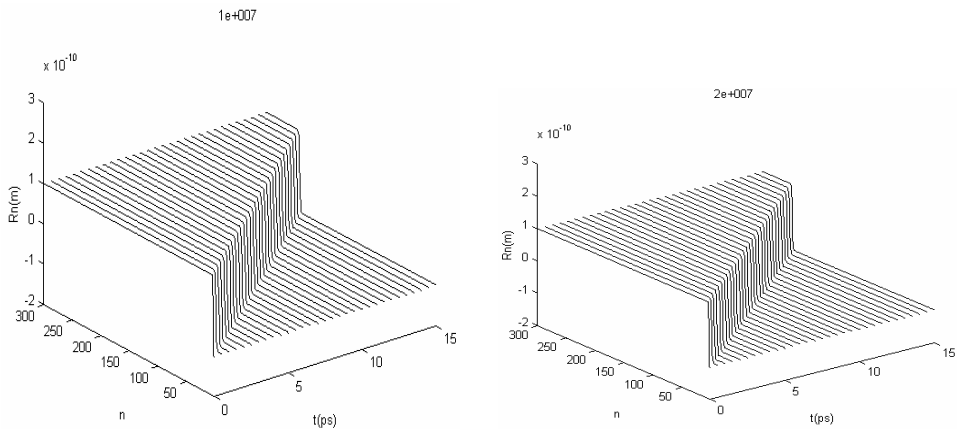

(a) (b)

Fig. 4. The features of the solitons at (a) $E = 100$ kV/cm and (b) 200 kV/cm at $T = \Gamma = 0$, respectively.

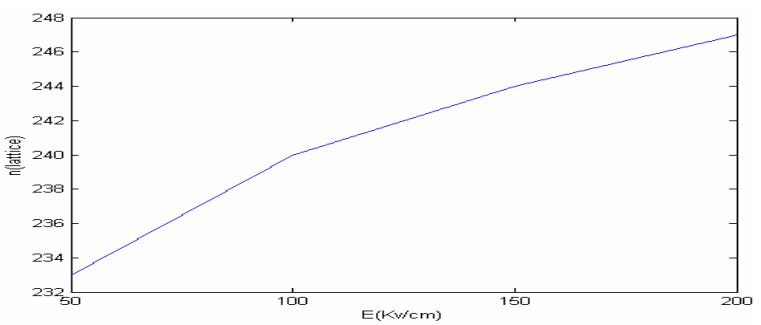

Fig. 5. This electric-field dependence of velocity of the soliton at $T = \Gamma = 0$, here the velocity is denoted by the lattice numbers passed in each second.

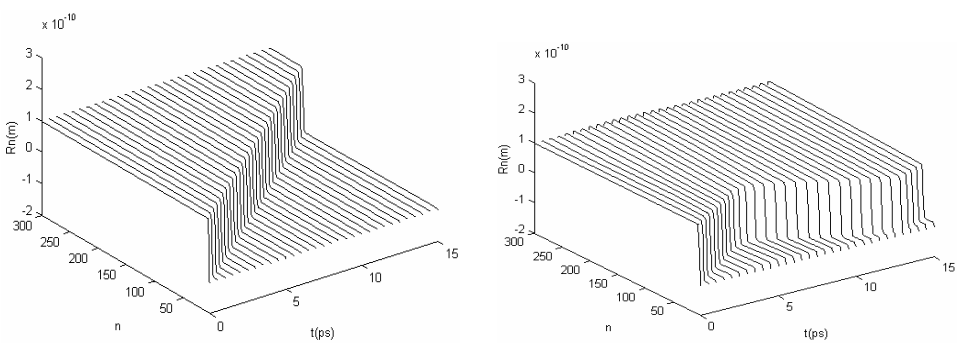

(a) (b)

Fig. 6. The properties of the new solitons, when the damping coefficients of medium are (a) $\Gamma = 5 \times 10^9$ s^{-1} and (b) 3×10^{11} s^{-1} at $T = E = 0$, respectively.

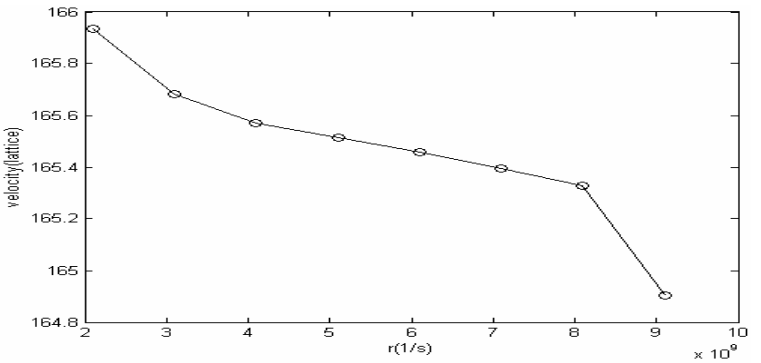

Fig. 7. The changes of velocity of soliton with variation of electric-field at $T = \Gamma = 0$, here the velocity is denoted by the lattice numbers pressed in each second.

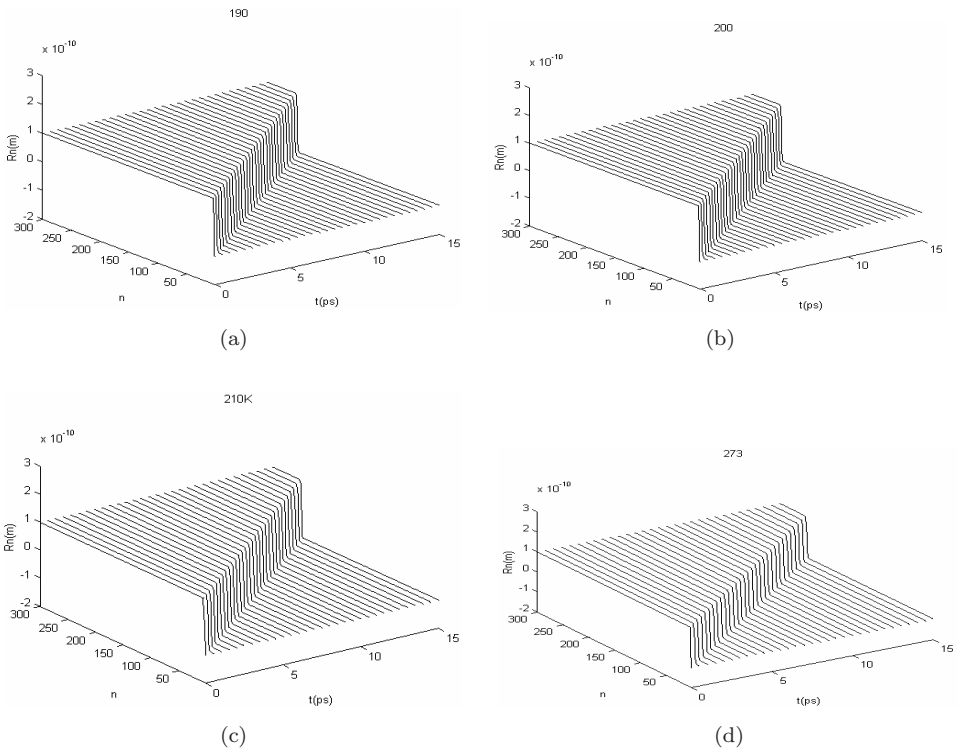

(a) (b) (c) (d)

Fig. 8. The features of soliton at different temperatures of (a) $T = 190$ K, (b) 210 K and (c) 273 K at $E = 200$ kV/cm and $\Gamma = 2 \times 10^9$ s^{-1} in the ice.

of these temperatures. This shows that the soliton is thermally stable at $T < 273$ K. Thus, the model of proton transfer in the ice crystal is available and successful.

From this simulation, we find that the motions of the proton-solitons accompanied by deformation of heavy ionic sublattices are initially accelerated under action

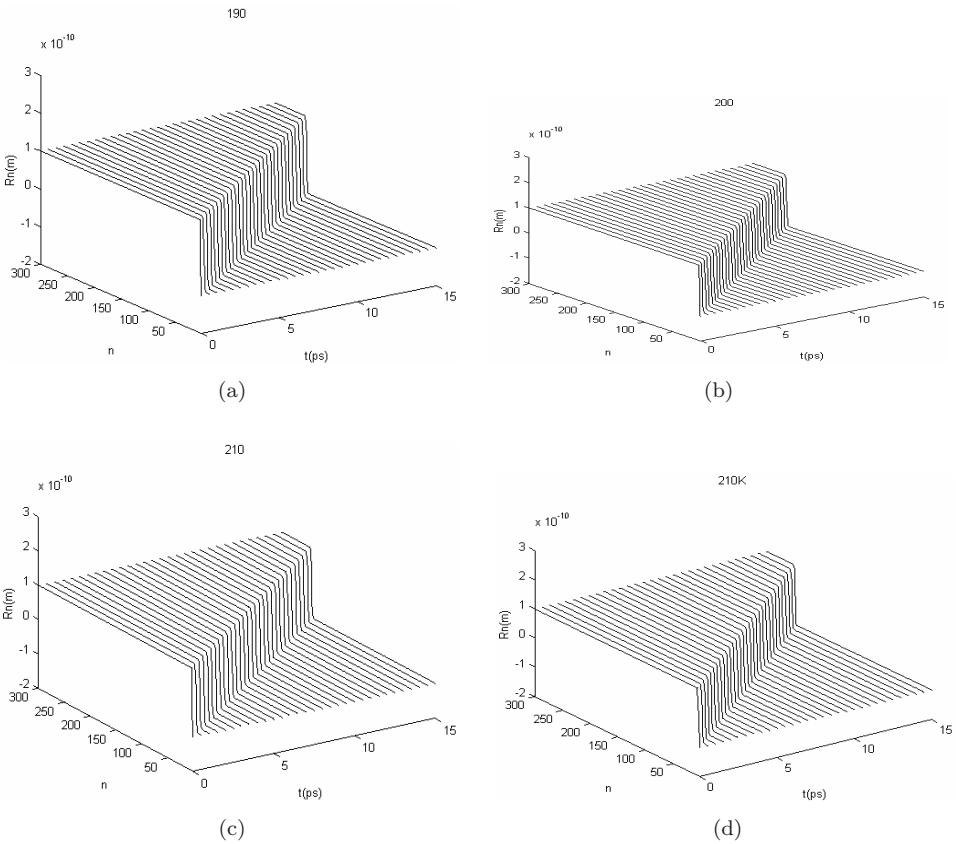

Fig. 9. The states of soliton at different temperatures of (a) $T = 190$ K, (b) 210 K and (c) 273 K at $E = 100$ kV/cm and $\Gamma = 2 \times 10^9$ s^{-1} in the ice.

of an externally applied field, when the temperature fluctuations of the systems produce a small random deviation. We also record the velocity of the proton-soliton conductivity at longer times, when the heavy ionic deformation complex moving with a constant velocity reaches a steady state. The results of numerical simulations for the mobility (or velocity) of the proton-soliton conductivity are shown in Figs. 10 and 11, in which we plot the terminal velocities of the proton-soliton conductivity as a function of inverse temperature for 200 kV/cm and 100 kV/cm in ice crystal, respectively. We see from these figures that the mobility of the proton-soliton conductivity increases with increasing temperature of medium, and has a peak to occur around 191.4 K. Subsequently it decreases, reaches a minimum at approximately 211.6 K, and then increases again. This behavior is very clear and basically the same for the two different electric-fields, although there are small differences in the details of two curves. Therefore the nonmonotonic up-down-up tendency of mobility of the proton-soliton in this region of temperatures seems to be a generic feature, and can also be observed for other electric-fields. We know from this study

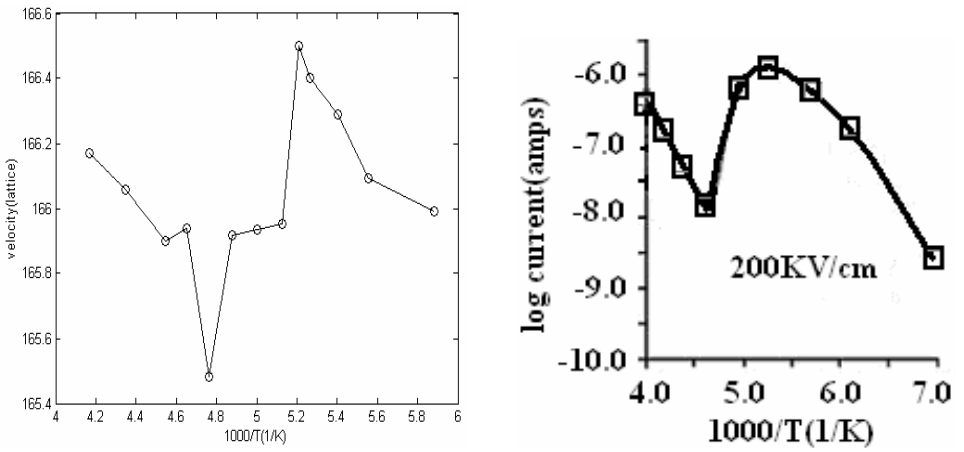

(a) (b)

Fig. 10. The inverse temperature-dependence of mobility (or velocity) for the proton conductivity at 200 kV/cm in ice, where (a) is calculated values, (b) is experimental values (Ref. 44 and 45).

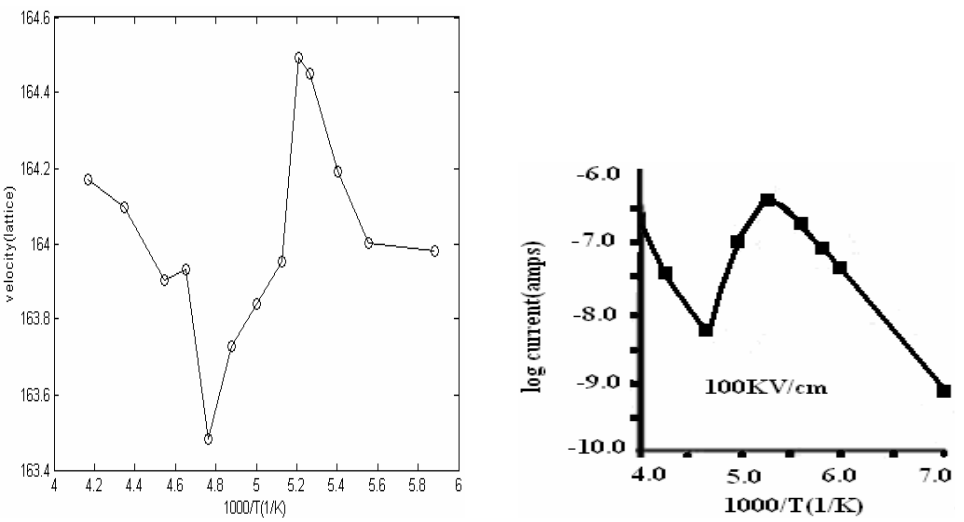

(a) (b)

Fig. 11. Changes of mobility (or velocity) of proton conductivity as a function of inverse temperature at 100 kV/cm in ice, where (a) is calculated values, (b) is experimental values (Ref. 44 and 45).

that the most distinct property of mobility-temperature plots in ice is the presence of two transition temperatures $T_{\max} = 191.4$ K and $T_{\min} = 211.6$ K, where the velocity of the proton-soliton conductivity reaches a maximum and minimum, respectively. The numerical simulation values in the new model are consistent with

the polycrystalline ice data shown in Fig. 10(b) and Figs. 11(b). In the latter, the same qualitative behavior also occurs, i.e., temperature-assisted mobility at lower temperatures and high temperatures with a very obvious drop in the intermediate range.

Nylund and Tsironis[35] early calculated the temperature-dependent mobility of proton transfer in the ice by the ADZ model; however, they obtained two minima in the changing curves of mobility (or velocity) with inverse temperature in the case of 100 kV/cm and different values of transition temperature from the above data, which are $T_{\max} = 190$ K and $T_{\min} = 210$ K, respectively. The results are all different from the experimental data shown in Figs. 10(b) and 11(b).

Obviously, the above feature of temperature-dependence of velocity of proton conductivity should directly attribute to the nonlinear interactions, the double-well potential and nonlinear coupling interaction, and to competition between the electric- field-induced biased proton motion and temperature effect in our model. In the absence of an electric-field, the potential of proton is symmetric around a central point which lies in the top of the potential barrier. When an electric-field is applied, the potential curve for the protons is distorted, thus the protons have a preferred direction of motion, which is just the direction of electric-field. Since the potential for the protons is nonlinear, then the motions of protons located at different double-well potentials in the hydrogen-bonded chains are not uniformly accelerated. When thermal motion is considered, an entire spectrum of Gaussian random displacements with a given temperature-dependent width is imposed upon the heavy ion lattice, its effects on the motion of protons located at different double-well potentials are different and are changed with variation of temperature of the systems. At lower temperatures, the protons which lie in the top of potential barrier have a more favorable attitude to cross over the barrier, when the electric-field is turned on. This behavior becomes increasingly likely with increasing temperature. In such a case the thermal fluctuations are just to push the protons towards the barrier as they are to pull it towards the bottom of potential well. Thus the velocity of the proton-soliton increases on the average because protons in the tops are more likely to cross over the barrier than other protons. Then the maximum of mobility (or velocity) of the proton-soliton can occur at the low temperatures. However, when the temperature continues to increase, the other protons located at other places in the double-well potentials can also cross the barrier more frequently, but their motions are easily hindered by the thermal perturbations of the systems due to the fact that their energies are smaller. Thus the velocity of the proton-soliton is reduced in this case. This behavior is much more pronounced with increasing temperature. When the temperature is so high that it can strongly hinder the motion of the proton-soliton, then the velocity of the proton-soliton can reach a minimum. However, its velocity increases again, once the soliton crosses over the barrier. This effect results in a minimum value of mobility of the proton-soliton to occur. Therefore, the nonmonotonic up-down-up tendency of mobility shown in

Figs. 10 and 11 is due to the combination effect of nonlinear double-well potential and thermal fluctuation and externally applied electric-field.

4. Conclusion

We here studied the dynamic properties of proton conductivity along the hydrogen-bonded molecular systems, for example, ice crystal, under the influences of the structure nonuniformity and thermal perturbation as well as damping of medium exposed in an externally applied electric-field by using a numerical simulation and fourth Runge–Kutta method in our model, where the quantum effect of proton has not been considered. The results obtained show that the proton-soliton is very robust against the structure nonuniformity including the fluctuation of force constant and disorder in the sequence of masses and thermal perturbation and damping of medium, the velocity of its conductivity increases by increasing the externally applied electric-field and decreasing the damping coefficient of medium, but the proton-soliton disperses at quite great fluctuation of the force constant and damping coefficient. In the numerical simulation, we find that the proton-soliton is thermally stable in the range of temperature of $T \leq 273$ K or 0°C under influences of damping and externally applied electric-field in the new model. In the meanwhile, the feature of nonmonotonic temperature-dependence with maximum at $T_{\max} = 191.4$ K and minimum at $T_{\min} = 211.6$ K for the mobility (or velocity) of the proton-soliton conductivity in the temperature region of 170–273 K is also obtained by the fourth-order Runge–Kutta method in our model. The nonmonotonic relation of change of mobility (or velocity) with increasing temperature and two transition temperatures obtained also agree with experimental data in ice crystals. The concordance between the experimental and theoretical data provides not only an evidence for real existence of the proton-soliton, which is possibly a real carrier of charge conductivity in ice crystal, but also demonstrate that the theoretical model of proton transfer is correct for the systems.

Acknowledgments

The authors would like to acknowledge the National "973" project of China for financial support (grant No: 212011CB503701).

References

1. P. Schuster, G. Zundel and C. Sandorfy, *The Hydrogen Bond, Recent Developments in Theory and Experiments* (North Holland, Amsterdam, 1976).
2. M. Peyrard, *Nonlinear Excitation in Biomolecules* (Springer, Berlin, 1995),
3. T. Bountis, *Proton Transfers in Hydrogen Bonded Systems* (Plenum Press, London, 1992).
4. M. Eigen and L. de Maeyer, *Proc. Roy. Soc. A* **247**, 505 (1958).
5. J. F. Nagle and S. T. Nagle, *J. Membr. Biol.* **74**, 1 (1983).
6. J. F. Nagle and H. J. Morowitz, *Proc. Natl. Acad. Sci. USA* **75**, 298 (1976).

7. V. Ya. Antonchenko, A. S. Davydov and A. V. Zolotaryuk, *Phys. Stat. Sol. (b)* **115**, 631 (1983).
8. St. Pnevmatikos, *Phys. Rev. Lett.* **60**, 1534 (1988).
9. A. V. Zolotaryuk and St. Pnevmatikos, *Phys. Lett. A* **142**, 233 (1996).
10. St. Pnermatikos, A. V. Savin, A. V. Zolotaryuk, Yu. S. Kivshar and M. J. Velgakis, *Phys. Rev. A* **43**, 5518 (1991).
11. St. Pnevmatikos, Yu. S. Kivshar, M. J. Velgakis and A. V. Zolotaryuk, *Phys. Lett. A* **173**, 43 (1993).
12. I. Chochliouros and J. Pouget, *Phys. Condensed Matter* **7**, 741 (1995).
13. R. Mittal and I. A. Howaed, *Physica D* **125**, 76 (1999).
14. A. V. Zolotaryuk, M. Peyrard and K. H. Spatschek, *Phys. Rev. E* **62**, 5706 (2000).
15. E. S. Nylund and C. P. Tsironis, *Phys. Rev. Lett.* **66**, 1886 (1991).
16. Y. Zolotaryuk and M. Salerno, *Phys. Rev. E* **73**, 066621 (2006).
17. Y. Zolotaryuk, M. Salerno and P. L. Christiansen, *Int. J. Mod. Phys. B* **17**, 4428 (2003).
18. A. V. Ustinov, C. Coqui, A. Kemp, Y. Zolotaryuk and M. Salerno, *Phys. Rev. Lett.* **93**, 087001 (2004).
19. X. F. Pang and H. J. W. Muller-Kirsten, *J. Phys. Condens Matter* **12**, 885 (2000).
20. X. F. Pang and Y. P. Feng, *Chem. Phys. Lett.* **373**, 392 (2003).
21. X. F. Pang and Y. P. Feng, *Chin. Phys. Lett.* **20**, 1071 (2003).
22. X. F. Pang and A. F. Jalbout, *Phys. Lett. A* **330**, 245 (2004).
23. X. F. Pang, H. W. Zhang and J. Zhu, *Int. J. Mod. Phys. B* **19**, 3835 (2005).
24. X. F. Pang and G. Zundel, *Acta Phys. Sin.* **46**(4), 625 (1997).
25. X. F. Pang and G. Zundel, *Chin. Phys.* **7**(1), 70 (1998).
26. X. F. Pang, *Chin. Phys.* **9**(2), 86 (2000).
27. X. F. Pang, *Prog. Phys. Sin.* **22**, 214 (2002).
28. X. F. Pang, *Phys. Stat. Sol. (b)* **238**, 43 (2002).
29. X. F. Pang, *Theory for Nonlinear Quantum Mechanics* (Chinese Chongqing Press, Chongqing, 1994), pp. 427–795.
30. X. F. Pang, *Soliton Physics* (Sichuan. Scie. Tech. Press, Chengdu, 2003), pp. 687–752.
31. X. F. Pang and Y. P. Feng, *Quantum Mechanics in Nonlinear Systems* (World Scientific Publishing Co., New Jersey, 2005), pp. 557–581.
32. X. L. Yan, R. X. Dong and X. F. Pang, *Commun. Theor. Phys.* **35**, 615 (2001).
33. J. Stiefel, *Einfuhrung in die Numerische Mathematik* (Teubner Verlag, Stuttgart, 1965).
34. K. E. Atkinson, *An Introduction to Numerical Analysis* (Wiley, New York, 1987).
35. P. S. Lomdahl and W. C. Kerr, *Phys. Rev. Lett.* **55**, 1235 (1985).
36. X. F. Pang, *Phys. Rev. E* **62**, 6989 (2000).
37. X. F. Pang, *European Phys. J. B* **19**, 297 (1999).
38. X. F. Pang, *Phys. Lett. A* **335**, 408 (2005).
39. X. F. Pang, *Commun. Theor. Phys.* **35**, 323 (2001).
40. X. F. Pang, *Commun. Theor. Phys.* **36**, 178 (2002).
41. X. F. Pang and Y. H. Luo, *Commun. Theor. Phys.* **41**, 470 (2004).
42. X. F. Pang and Y. H. Luo, *Commun. Theor. Phys.* **43**, 367 (2005).
43. X. F. Pang, H. W. Zhang and Y. H. Luo, *J. Phys. Condensed Matter* **18**, 613 (2006).
44. P. B. Hobbs, *Ice Physics* (Clarendon, Oxford, 1974).
45. H. Engelheart, B. Bullemenr and N. Riehl, in *Physics of Ice*, eds. N. Reihl, B. Bullemer and H. Engelheart (Plenum, New York, 1969).